Chemosphere 240 (2020) 124850

Contents lists available at ScienceDirect

Chemosphere

journal homepage: www.elsevier.com/locate/chemosphere

Lung surfactant monolayer – A good natural barrier against dibenzo-*p*-dioxins

Anna Stachowicz-Kuśnierz [a, **], Tomasz Seidler [a], Ewa Rogalska [b], Jacek Korchowiec [a], Beata Korchowiec [c, *]

[a] Department of Theoretical Chemistry, Faculty of Chemistry, Jagiellonian University, ul. Gronostajowa 2, 30-387, Krakow, Poland
[b] UMR 7053 CNRS-UL, Université de Lorraine, Faculté de Sciences et Technologies, B.P. 70239, 54506, Vandoeuvre-lès-Nancy cedex, France
[c] Department of Physical Chemistry and Electrochemistry, Faculty of Chemistry, Jagiellonian University, ul. Gronostajowa 2, 30-387, Krakow, Poland

HIGHLIGHTS

- DD and 2CLDD molecules accumulate in the hydrophobic part of LS model membranes.
- Both dioxins have a common condensing influence on the lipids.
- LS may be recognized as a good barrier for uncontrolled uptake of airborne dioxins.
- Presence POPC reduces harmful effects of small, hydrophobic pollutants on LS system.

GRAPHICAL ABSTRACT

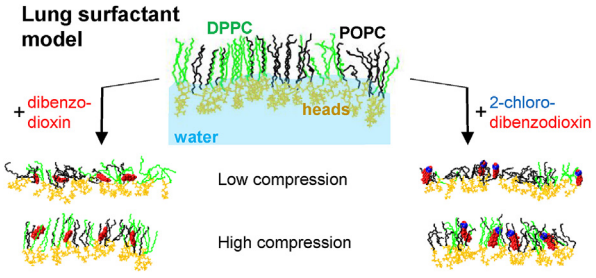

ARTICLE INFO

Article history:
Received 11 July 2019
Received in revised form
27 August 2019
Accepted 12 September 2019
Available online 18 September 2019

Handling Editor: Jian-Ying Hu

Keywords:
Lung surfactant
Air pollution
Dibenzo-*p*-dioxin
2-Chlorodibenzo-*p*-dioxin
II-A isotherms
PM-IRRAS
Molecular dynamics

ABSTRACT

The present study deals with interaction of two air pollutants: dibenzodioxin, DD, and its' monochlorinated derivative, 2-chlorodibenzodioxin, 2CLDD, with models of the lung surfactant (LS) system. A monolayer composed of DPPC and POPC in 1:1 molar ratio was used as a model of LS. One component monolayers of DPPC and POPC were also examined, to model the interiors of LC and LE domains in LS, respectively. Molecular dynamics simulations and measurements of surface pressure isotherms, as well as polarization modulation-infrared reflection-absorption spectra were employed to study the influence of dioxins on the monolayers. We demonstrate, that both dioxins adsorb and accumulate in the hydrophobic parts of all three monolayers. DD molecules prefer flat orientation on the surface at large areas. Upon compression, they lift and orient perpendicularly to the monolayer. Flat orientation of DD molecules leads to their large surface area. In consequence they preferentially locate in vicinity of unsaturated chains of POPC – they are small enough to fill void spaces created by kinks in unsaturated chains. 2CLDD orient along monolayer normal already at the largest areas and preference for POPC was not observed for them. In laterally relaxed states, a condensing effect, connected with reduction of surface area available to the lipids was observed for both dioxins. In the case of 2CLDD, additional locally ordering influence of dioxin molecules was detected. In compressed states, the presence of dioxin molecules hinders alignment and uniform ordering of lipid chains.

1. Introduction

In air-breathing animals effective gas exchange requires large surface of contact between the ambient air and blood. It is covered

* Corresponding author.
** Corresponding author.
E-mail addresses: stachowa@chemia.uj.edu.pl (A. Stachowicz-Kuśnierz), bkorch@chemia.uj.edu.pl (B. Korchowiec).

https://doi.org/10.1016/j.chemosphere.2019.124850

with a thin layer of aqueous medium, leading to a large area of air-water phase boundary. Due to large surface tension of water, sustaining this surface and expanding it at inhalation would require a large amount of energy. In order to reduce surface tension, the interface is covered with a surface active material - lung surfactant (LS), which forms a monolayer on the interface, and consequently reduces the work of breathing and prevents alveolar collapse at the end of exhalation.

In most mammalian species LS is primarily composed of phospholipids (85 wt%) (Veldhuizen et al., 1998). Among them, phosphatidylcholine (PC) is the most abundant (70–85 wt%) (Goerke, 1998). About 50 wt% of the total PC pool is the disaturated dipalmitoylphosphatidylcholine (DPPC). The remaining 50% contains PC with either mono- or diunsaturated alkyl chain in the *sn*-2 position (Serrano and Perez-Gil, 2006). Other lipids present in LS include anionic phosphatidylglycerol and phosphatidylinositol, phosphatidylethanolamine, and cholesterol. LS also contains *c.a.* 10 wt% of surfactant-associated proteins (Orgeig et al., 2010). They belong to two groups: hydrophilic proteins, which reside in the aqueous subphase and take part in innate defense mechanisms (Perez-Gil, 2008), and hydrophobic proteins, which are associated with the lipids. Hydrophobic proteins are crucial for surface activity of LS. They assist initial lipid adsorption and their cycling between the surface and 3-dimensional surface-associated reservoirs (Duncan and Larson, 2010).

In the equilibrium state, the presence of LS reduces surface tension, γ, to an equilibrium spreading value of $\gamma_{eq} = 20–27\ mN\ m^{-1}$ (Veldhuizen et al., 1998). However, during breathing cycles alveolar surface area oscillates in the range of 25–30%, resulting in alternate compression/decompression of LS. This process is accompanied by γ changes between $\approx 30\ mN\ m^{-1}$ at full inhalation to $\approx 0\ mN\ m^{-1}$ at the end of exhalation (Schurch et al., 1976; Schürch, 1982). The exact mechanism of this process is still under debate (Piknova et al., 2001; Engelskirchen, 2007). According to, the most commonly accepted, modified squeeze-out model (Zhang et al., 2011; Keating et al., 2012), LS reaches near zero surface tension by forming a highly ordered liquid condensed (LC) phase. At physiological temperature, this is only possible for DPPC, since other lipids are above the critical temperature for the phase transition. In native surfactants, existence of LC domains, composed mainly of DPPC, embedded in a disordered liquid expanded (LE) phase has been confirmed experimentally (Zuo et al., 2008). LE phase contains mostly unsaturated and anionic lipids, as well as hydrophobic proteins. During compression/decompression LE phase cycles between the surface and a network of multi-layered 3D structures associated with the interface.

The current study focuses on interactions between a lung surfactant model lipid system and two air pollutants potentially harmful to it, namely: dibenzo-*p*-dioxin, DD, and its monochlorinated derivative, 2-chlorodibenzo-*p*-dioxin, 2CLDD (Scheme S1 and Table S1 in Supplementary Materials). Polychlorinated derivatives of DD (PCDD) constitute a class of dangerous environmental pollutants of mainly anthropogenic origin (Kulkarni et al., 2008; Dopico and Gomez, 2015). Their most important source in the atmosphere are combustion processes, such as: municipal and medical waste incineration, backyard burning of waste, and open fires. Toxicity of PCDDs is well documented (White and Birnbaum, 2009; Tavakoly Sany et al., 2015) and their release has been greatly limited thanks to technological progress and regulations imposed on industry (Comission, 2001; Davy, 2004). However, little attention is payed to the low chlorinated derivatives of DD (mono-to trichlorinated DD, LCDDs). The reason for that is their relatively low toxicity, as compared to compounds with four or more chlorine atoms. Unlike PCDDs, LCDDs do not bind to the aryl hydrocarbon receptor (AhR), therefore their international Toxic Equivalent Factors are zero (Van den Berg et al., 2006). According to IARC (International Agency for Research on Cancer) classification of chemical compounds, DD is considered “not classifiable as to its carcinogenicity to humans” (group 3) (World Health Organization, 1997). Nevertheless, LCDDs can still be deleterious to the LS system. The levels of LCDDs released in combustion processes are comparable to those of PCDDs (Gullett and Wikstrom, 2000; Liu et al., 2013). Yet, decreasing the number of Cl atoms increases volatility of DDs and reduces their deposition on ash particles. Therefore, larger amounts of LCDDs can be released to the atmosphere, as compared to PCDDs. Recent studies have confirmed that LCDDs can dominate over PCDDs in ambient air samples (Zhang et al., 2016), and that they can travel long distances in the atmosphere (Han et al., 2016).

Dioxins are known for their hydrophobicity and tendency to accumulate in fatty matter. Therefore, it can be expected that they interact strongly with LS lipids and amass on the surface. In our previous studies we have demonstrated that such impurities can perturb phase behavior of lipid monolayers (Korchowiec et al., 2008, 2011, 2016a, 2016b; Stachowicz-Kusnierz et al., 2017). The effect can be either ordering or disordering. In the first case, highly ordered domains emerge in the vicinity of foreign molecules. In the second, pollutant disturbs lipid packing and often precludes formation of LC phase. Both of these effects can lead to changes in mechanical properties of LS, and in consequence to its malfunctioning and respiratory disorders.

2. Materials and methods

2.1. Materials and reagents

The chemical structures of the compounds employed in this study are shown in Scheme S1. Synthetic 1,2-dipalmitoyl-*sn*-glycero-3-phosphocholine (DPPC) and 1-palmitoyl-2-oleyl-*sn*-glycero-3-phosphocholine (POPC) (all >99% pure) were purchased from Avanti Polar Lipids. Dibenzo-*p*-dioxin (DD) and 2-chlorodibenzo-*p*-dioxin (2CLDD) (both >99% pure) were from AccuStandard. Spectrophotometric grade chloroform (99.9% pure), used for preparing solutions, was purchased from Sigma-Aldrich. Ultrapure water (Milli-Q, Millipore) with resistivity of 18 MΩ cm and a surface tension of $72.8\ mN\ m^{-1}$ at 20 °C, (pH 5.6) was used as subphase.

2.2. Surface pressure measurement

The surface pressure (Π) measurement was carried out with a KSV 2000 Langmuir balance (KSV Instruments, Helsinki, Finland). A Teflon trough (58 × 15 × 1 cm) with two hydrophilic Delrin barriers providing a symmetric compression was used in all experiments. Surface pressure measurements were carried out using the Wilhelmy plate method. The apparatus was closed in a Plexiglas box and the temperature was kept constant at 25 °C. Before each measurement, the trough and the barriers were cleaned using cotton soaked in chloroform, then ethanol and then rinsed with Milli-Q water. All impurities were removed from the subphase surface by sweeping and suction. The surface pressure – area (Π-A) isotherms were measured for lipid monolayers, 1:1 binary mixture of DPPC and POPC, as well as their mixtures containing 0.1 mol fraction of DD or 2CLDD. The monolayers were spread from calibrated solutions of accurate concentrations ($0.5\ mg\ mL^{-1}$) using a microsyringe (Hamilton Co., USA). After the equilibration time of 20 min, the films were compressed at the rate of $5\ mm\ min^{-1}$ by two symmetrically moving barriers. A PC computer and KSV software were used to control the experiments. Each compression isotherm was performed at least three times. The subphase temperature was maintained constant using Lauda RE 104 thermostat.

The standard deviation obtained from compression isotherms was ±0.5 Å^2 on mean molecular area (A), and ±0.2 mN m^{-1} on surface pressure.

2.3. Polarization–modulation infrared reflection–absorption spectroscopy

The PM-IRRAS spectra of pure 1:1 binary mixture of DPPC and POPC, as well as the mixture containing 0.1 mol fraction of DD or 2CLDD spread on water subphase were acquired at 25 °C. The PM-IRRAS measurements were performed using a KSV PMI 550 instrument (KSV Instruments Ltd., Helsinki, Finland). A detailed description of the experimental set up can be found in our previous paper (Czapla et al., 2011). The PM-IRRAS spectra of the film-covered surface, $S(f)$, as well as that of the pure water, $S(w)$, were measured and the normalized difference $\Delta S/S = [S(f) - S(w)]/S(w)$ is reported. In total, 6000 interferogram scans (10 scans per second) have been acquired for each spectrum. The spectral range of the device is 800–4000 cm^{-1}, and the resolution is 8 cm^{-1}.

2.4. Molecular dynamics simulations

LS models were prepared as two monolayers of 100 lipids distributed on a regular rectangular grid. A slab of 30 000 water molecules was placed between them. These structures were equilibrated via energy minimization, followed by 10 ns of NVT simulation at 298 K. Further, the systems were simulated at constant temperature (298 K), normal pressure (1 bar), and surface tension target ranging from 120 to 0 mN m^{-1}. From these simulations, systems with mean molecular area (MMA) of 1.00, 0.90, 0.80, 0.70 and 0.60 nm^2 molecule^{-1} (corresponding to total surface area of 100, 90, 80, 70, and 60 nm^2) were selected. For DPPC additional area of 0.55 nm^2 molecule^{-1} (surface area 55 nm^2) was also selected, to account for the highly compressed states obtained for this lipid at large surface pressures. For every system, 10 mol%, *i.e.* 11 dibenzo-*p*-dioxin molecules, was introduced into each monolayer and NVT (at 298 K) equilibration was performed for 20 ns. Based on selected snapshots, DD molecules were changed to 2CLDD by replacing hydrogen atom at position 2 with chlorine. All the systems, including those without impurities, were then subject to 25 ns of NVT equilibration at 298 K and 100–200 ns of production simulation. In production runs stabilization of surface tension was used as a termination criterion. Surface tension was computed with the formula:

$$\gamma = \frac{l_z}{2}\left(p_{zz} - \frac{p_{xx} + p_{yy}}{2}\right) \quad (1)$$

where l_z is the height of the simulation box, and p_{ii} are the diagonal pressure tensor components in the direction normal (p_{zz}), and lateral (p_{xx}, p_{yy}) to the monolayer. Standard deviations of the γ values were within 6 mN m^{-1}. Such large values are inherent to the adapted protocol of the surface tension calculation. Π-A isotherms were constructed with the use of surface pressure, Π, defined as:

$$\Pi = \gamma_o - \gamma \quad (2)$$

where γ_o is the surface tension of pure water subphase. An experimental value of 72 mN m^{-1} was adopted for γ_0 (Vargaftik et al., 1983).

Preparatory simulations were performed with NAMD (Phillips et al., 2005) program, while production runs were done in Gromacs 2018 (Abraham et al., 2015). All-atom CHARMM36 force fields were used for lipids (Klauda et al., 2010) and dibenzo-*p*-dioxin (Vanommeslaeghe et al., 2010) molecules, whereas 4-point OPC model (Izadi et al., 2014) was used for water. Such combination of force fields was recently shown to yield a very good agreement between calculated and experimental Π-A isotherms for DPPC and POPC (Javanainen et al., 2018). Dioxin molecules were parametrized according to procedure described in Mayne et al. (2013), using the graphical force-field toolkit available in VMD package (Humphrey et al., 1996). The procedure included geometry optimization at MP2/6-31G* level of theory, fitting of atomic charges, based on the energies of interaction with water molecules, and fitting of the missing dihedral angle parameter between oxygen atoms (1,4-dioxin bridge). The charges obtained for chlorine atoms were split into the core charge and the lone pair region, corresponding to the sigma hole (Soteras Gutierrez et al., 2016). The sigma hole charge was fixed at 0.05 e and positioned at 0.164 nm from the chlorine atom. The remaining charge of the carbon-chlorine group was distributed in such way that reproduced the molecular dipole moment, derived from the original molecular geometry and remaining atomic charges. The quantum-chemical calculations were performed with Gaussian 09 package (Frisch et al., 2009). In all simulations periodic boundary conditions were applied in all three directions. In order to eliminate unphysical interactions between replicas in the direction perpendicular to the monolayers (z) the box length in this direction was increased to 100 nm. In preparatory simulations, Langevin thermostat and barostat (Feller et al., 1995) were used to control the temperature and pressure. Production simulations were carried out in NVT ensemble, with velocity rescaling applied to control the temperature. A time-step of 1 fs was used in preparatory simulations. In production runs it was increased to 2 fs and all bond lengths involving hydrogen atoms were frozen at equilibrium values with the use of LINCS algorithm (Hess et al., 1997). In all simulations 1.2 nm cut-off was used for van der Waals interactions and full electrostatics was calculated with PME method (Darden et al., 1993).

Trajectories were visualized with VMD package (Humphrey et al., 1996). Trajectory analysis was performed with home-developed programs, VMD, and Gromacs tools. All computed properties were averaged over the two monolayers present in each system. The only exception were the density profiles along monolayer normal. Deuterium order parameters were calculated with a home developed program according to the formula:

$$S_{mol} = -2S_{CD} \quad (3)$$

$$S_{CD} = \frac{1}{2}\left(3 < \cos^2\theta > - 1\right) \quad (4)$$

where θ is the angle between C–H bond and monolayer normal and <> denote averaging over time, molecules, and both C–H bonds formed in each CH_2 group. *rdf*, *density*, *gangle* and *msd* tools from Gromacs were applied to calculate radial pair distribution functions, $g(r)$, density profiles along monolayer normal, tilt angles between various system components and monolayer normal, and diffusion coefficients, respectively. Headgroups hydration was calculated from three-dimensional radial pair distribution functions. For each of the atoms of interest the position of the first minimum in the $g(r)$ curve was located. The number of water molecules was then determined as the value of integrated $g(r)$ up to this point. Similar procedure was employed in the calculation of average number of carbon atoms from lipid chains in the first coordination shell of dioxin molecules.

3. Results and discussion

LS model employed in this study was composed of DPPC and POPC (Scheme S1) in 1:1 molar ratio. One-component monolayers

of DPPC and POPC, with and without foreign molecules, were also studied to model interiors of LC and LE domains in LS, respectively. The influence of impurities on global properties of the monolayers were studied by means of surface pressure-area (Π-A) isotherms. Additional detailed information was obtained from PM-IRRAS measurements and atomistic molecular dynamics (MD) simulations at varying surface areas. The concentration of 10 mol% was chosen for DD and 2CLDD molecules. This is a rather high value, but allows us to elucidate clear trends in the influence of impurities on the monolayers. Moreover, since dioxins accumulate in lipids, such concentrations can be reached in real systems upon long-time exposures. In summary, nine systems were examined. They include three lipidic compositions of the monolayer: DPPC, POPC, and their 1:1 mixture (MixPC). The systems without dioxin molecules will be referred to as pure DPPC, POPC, and MixPC monolayers. The remaining six systems include three monolayers with DD molecules (DPPC + DD, POPC + DD, MixPC + DD) and three monolayers with 2CLDD molecules (DPPC+2CLDD, POPC+2CLDD, MixPC+2CLDD).

3.1. Surface pressure isotherms

Global physicochemical properties of monolayers of surface active species are routinely examined via surface pressure-area isotherms. Reproduction of experimental isotherms can also be regarded as a good criterion for assessing the quality and reliability of results obtained from simulations of Langmuir monolayers. In order to compare simulated surface tensions at varying mean molecular area (MMA) with experimental isotherms, the former have to be converted into surface pressures (Π). This requires adoption of a specific value for the surface tension of water (γ_0, see equation (2)), which can sometimes be problematic due to known problems of common MD force fields with reproducing the experimental value for γ_0 (Vega and de Miguel, 2007; Zakharov et al., 1998). For this reason, in the present study the 4-point OPC model was employed for water. This model was recently shown not to suffer from the above drawback and allows employment of experimental value for $\gamma_0 = 72$ mN m^{-1} (Javanainen et al., 2018). Fig. 1 presents experimental and calculated Π-A isotherms obtained in this study, together with some literature data available for monolayers without dioxins. In panels (a) and (b) of Fig. 1 isotherms for one component monolayers of pure DPPC and pure POPC are presented. It can be seen that for DPPC monolayer experimental results available in the literature show large discrepancies, which may be connected with various experimental details, such as the type of experimental apparatus, choice of spreading solvent or different mode and rate of compression. It has been shown that these factors can have a large impact on the stability of DPPC monolayers on the air-water interface and hence the isotherms (Munden and Swarbrick, 1973; Goerke and Gonzalez, 1981; Wüstneck et al., 2000; Duncan and Larson, 2008). From this point of view, agreement between the isotherm calculated in this study and literature data can be considered as satisfactory. Qualitative reproduction of the plateau corresponding to the transition from LE to LC phase can be seen. Except for the point corresponding to 0.70 nm^2 molecule^{-1}, calculated surface pressures agree well with the isotherms of Olzynska et al. (2016) and Eftaiha et al. (2012). At 0.70 nm^2 molecule^{-1} the agreement is slightly worse. The same behavior was observed in the simulations of Javanainen et al. (2018) who explain it with hampered equilibration of the system in the

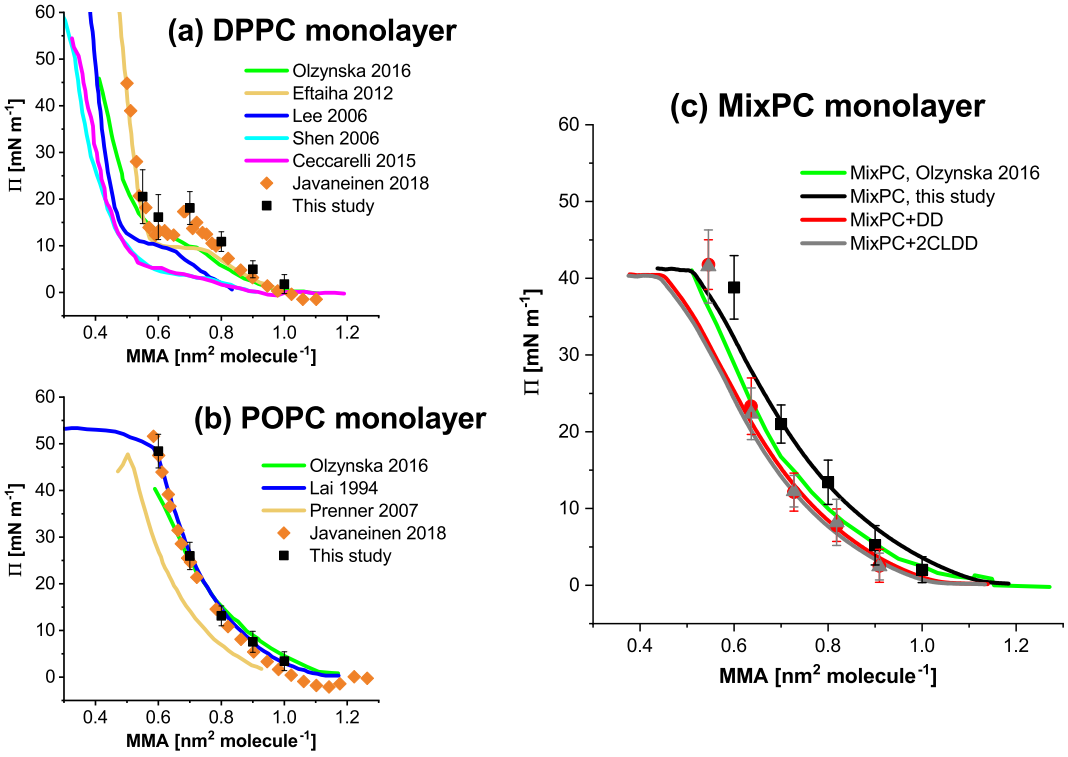

Fig. 1. Left: calculated Π-A isotherms obtained in this study (black points) for pure DPPC (a) and pure POPC (b) monolayers compared with experimental and simulated isotherms from the literature. Literature data is taken from references: Lai et al. (1994), Lee et al.(2006), Shen et al. (2006), Prenner et al. (2007), Eftaiha et al. (2012), Ceccarelli et al. (2015), Olzynska et al. (2016), Javanainen et al. (2018). Right: (c) Calculated (points) and experimental (lines) Π-A isotherm for MixPC (black), MixPC + DD (red), and MixPC+2CLDD (grey) systems obtained in this study together with literature data from Olzynska et al. (2016) (green line). In all panels experimental isotherms are drawn with lines and simulated isotherms are shown with points. All isotherms correspond to 298 K and pure water subphase. In the calculated isotherms a value of 72 mN m^{-1} was adopted for the surface tension of water.

MMA region close to the phase transition. In the case of POPC monolayer, the agreement between the calculated and experimental surface pressures is very good. The results obtained here agree with experimental results of Olzynska et al. (2016) and Lai et al. (1994) in the whole MMA range. The experimental isotherm of Prenner et al. (2007) clearly differs from other experimental and computational results, which is probably due to differences is experimental setup (Huynh et al., 2014).

Panel (c) of Fig. 1 shows experimental and calculated isotherms for the MixPC, MixPC + DD and MixPC+2CLDD systems obtained in this study. Experimental isotherm recorded by Olzynska et al. (2016) for MixPC is also shown for comparison. The agreement between experimental and calculated results is reasonably good. Except for the smallest MMA, surface pressures obtained from the simulations are close to experimental curves. Deviations between calculated and experimental values are within the error bars for the simulated surface pressures. At the lowest MMA, calculated Π values are overestimated with respect to the experiment, suggesting that the simulated systems are in a meta stable state. The reason for this behavior is probably connected with coexistence of LC and LE domains in the monolayers. Due to limited size and time scale of the calculations this effect could not be captured in all-atom MD simulations.

Both calculations and experimental measurements show that the isotherm of MixPC system is shifted towards smaller MMA upon addition of both DD or 2CLDD. Similar effect of the presence of dioxin molecules was observed in the simulations of DPPC and POPC systems with and without those impurities (the isotherms are presented in Fig. S1 of the Supplementary Materials available for this article). Such shift of the isotherms shows that the presence of dioxins has an ordering influence on the monolayers. In general, the influence of foreign molecules on ordering of lipid chains can be connected with two effects. The first one is a condensing effect, related to reduction of surface area available to the lipids. It results in lipid compression and increased ordering. The second is connected with perturbation of local environment of the chains, arising from the presence of foreign molecules. Depending on the nature of impurities, this effect can be either ordering, or disordering. In what follows we will try to elucidate which of the above effects dominates in the interactions between lipids and dioxin molecules adsorbed in the monolayers.

3.2. MD simulations

Results obtained for monolayers without dioxins (pure DPPC, pure POPC and MixPC systems) are similar to those reported in other MD studies of phospholipid monolayers (Baoukina et al., 2007; Huynh et al., 2014; Olzynska et al., 2016; Javanainen et al., 2018). Snapshots from simulations of these systems are gathered in Fig. S2 of Supplementary Materials. In brief, depending on MMA, LE and LC phases can be observed in those monolayers. In our previous simulations, employing TIP3P water model (Jorgensen et al., 1983), in pure DPPC and MixPC systems gaseous (G) phase was also observed at MMA 1.00–0.90 nm^2 $molecule^{-1}$ (corresponding to surface areas of 100 and 90 nm^2, respectively). There is some debate in the literature whether pore formation at these relatively small MMA values is a physical effect or an artifact of the force field (Roke et al., 2003; Knecht et al., 2005; Baoukina et al., 2007; Duncan and Larson, 2008; Nisoh et al., 2015). In this study we observe that, in line with the findings of Javanainen et al. (2018), improved reproduction of γ_0 in the OPC water model results in pore closure and both pure DPPC and MixPC monolayers are continuous and entirely in LE phase at MMA from 1.00 to 0.70 nm^2 $molecule^{-1}$, *i.e.* surface areas from 100 to 70 nm^2 (Fig. S2a and S2e).

Due to bulky character of the lipid, pure POPC monolayer is in LE phase at all surface areas examined here (100–60 nm^2, MMA = 1.00–0.60 nm^2 $molecule^{-1}$). It is characterized by disordered conformations of lipid chains, with large number of gauche defects. Pure DPPC monolayer undergoes a phase transition to LC phase at surface area between 70 and 60 nm^2 (MMA = 0.70–0.60 nm^2 $molecule^{-1}$) – number of gauche defects gradually decreases and clusters of highly ordered lipid chains are formed (70 nm^2) and grow (60 nm^2). At 55 nm^2 DPPC monolayer is entirely in LC phase (Fig. S2d). Alkyl chains adopt all-trans conformations and tilt uniformly in the same direction. Most populated tilt angle with respect to the monolayer normal is equal to 38°. MixPC monolayer exhibits an intermediate behavior between the two one-component systems. At surface areas from 100 to 70 nm^2 it is in LE phase. At 60 nm^2 small, highly ordered clusters of DPPC, surrounded with more disordered LE phase can be observed (Fig. S2f). This can be regarded as initial stages of phase separation observed both experimentally and in large-scale MD simulations for mixed monolayers of DPPC with unsaturated phospholipids (Baoukina et al., 2012; Keating et al., 2012). Pure LC phase is not formed in this system, due to the presence of unsaturated chain in POPC.

Eye examination of the trajectories obtained for the systems containing DD and 2CLDD reveals that both dioxins readily adsorb in the hydrophobic part of the monolayers, in accordance with their known lipophilic character. Even at the largest compressions, we did not observe escape of dioxin molecules from the surface, neither to the subphase, nor vacuum. However, behavior of DD and 2CLDD and their influence on the monolayers is different, especially at large surface areas.

3.2.1. Monolayers with DD molecules

Eye examination of the recorded trajectories (selected representative snapshots are gathered in Fig. S3 of Supplementary Materials) reveals that at large surface areas, *i.e.* 100–80 nm^2, DD molecules lie flat on the boundary between hydrophilic and hydrophobic parts of all three monolayers. As surface pressure in the monolayers increases, they lift up and attain an orientation in which their long molecular axis is roughly perpendicular to monolayer plane. These observations were confirmed by distributions of tilt angles between long molecular axis of DD and monolayer normal (Fig. 2). For all three systems a maximum around 90° can be observed in weakly compressed states, demonstrating that dioxin molecules preferentially orient flatwise on the interface. Such orientation most probably results from entropic factors, *i.e.* it allows to maintain high entropy of tangled lipid chains. It results in large surface area of DD molecules.

Upon compression dioxin molecules lift up - maxima in tilt angle distributions move towards smaller values. In POPC + DD and MixPC + DD monolayers at 60 nm^2 the most populated tilt angle of DD equals to 23–25°. In DPPC + DD system at 60 and 55 nm^2 DD molecules tilt together with surrounding lipid chains, and the maximum of tilt angle distribution appears at a larger value of 35–38°. In these highly compressed states of DPPC + DD system DD molecules form linear structures in which they line up and tilt uniformly in the same direction as the lipid chains (Fig. S3d and S3g). In this way the disturbing influence of DD presence on the monolayer is minimized. However, as will be shown below, presence of DD molecules still perturbs the monolayer to some extent, because uniform tilt of the lipid chains is hindered.

In order to examine the location of DD molecules in the monolayers density profiles along monolayer normal for various system components X, $\rho_X(z)$, can be examined. Examples of such profiles are shown in Fig. S4 of Supplementary Materials. A closer look at panels (a-c) of Fig. S4 reveals that at low compression DD molecules embed deeper in the hydrophobic region of monolayers

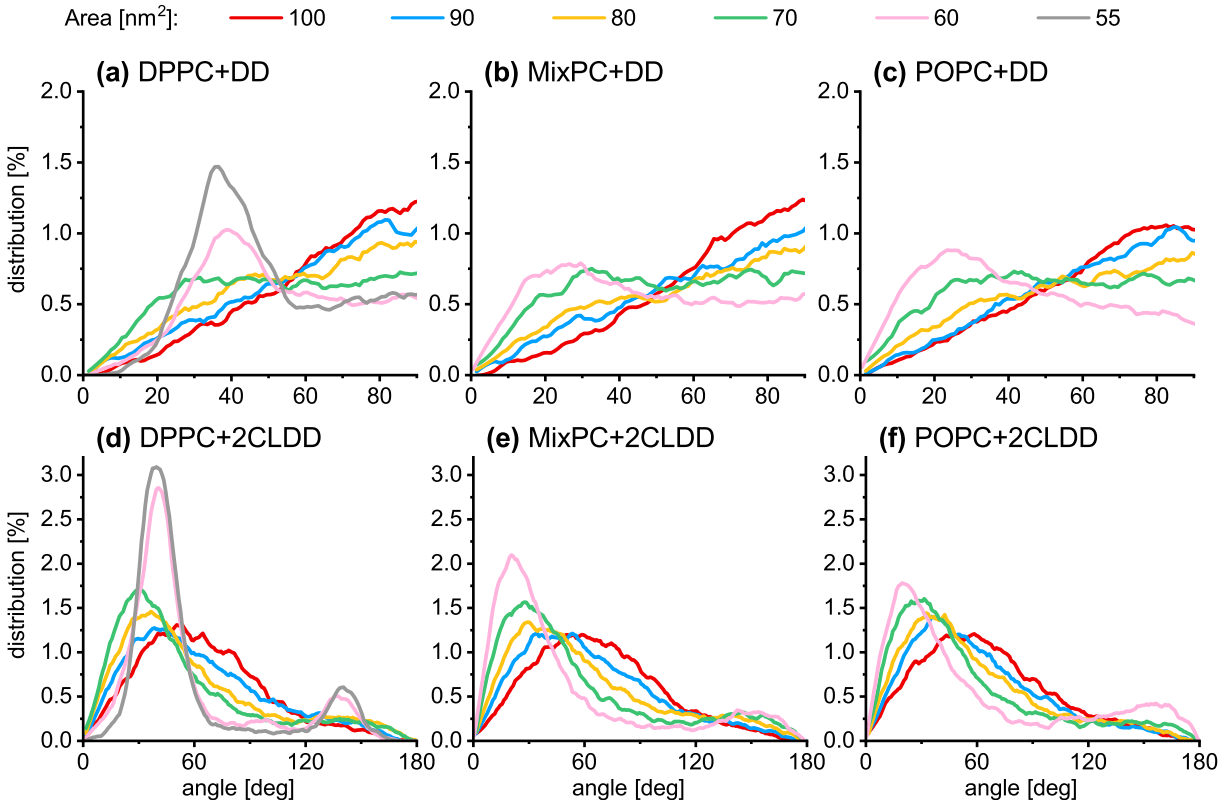

Fig. 2. Distribution of tilt angles between long molecular axis of dioxin molecules and monolayer normal. Top row: results for systems with DD molecules, bottom row: results for systems with 2CLDD molecules. In systems containing 2CLDD, molecular axis is directed towards Cl atom. The curves have been subject to signal smoothing for clarity.

containing POPC than in the DPPC + DD monolayer. This observation can be quantified by integrating the area under this part of the density profile of dioxin molecules, $\rho_{DD}(z)$, which does not overlap with the density of water. The results of such calculation are shown in Fig. 3a. It can be seen that at areas between 100 and 80 nm^2 DD molecules reside deeper in POPC + DD monolayer than in DPPC + DD monolayer, with MixPC + DD system exhibiting an intermediate behavior. The explanation for this behavior comes from interplay of two factors. Firstly, due to favorable van der Waals interactions, in DPPC monolayers saturated lipid chains align temporarily even at large surface areas. This effect is smaller in monolayers containing POPC due to presence of a double bond in *sn*-2 chain of POPC. *Sn*-2 chains of POPC are kinked which results in presence of empty spaces at the interface in monolayers containing POPC. Secondly, spatial dimensions of DD molecules are comparable to both "halves" of *sn*-2 chain of POPC, *i.e.* the two parts of *sn*-2 chain before and after the double bond. Namely, average dimensions of a DD molecule (measured as the distance between the

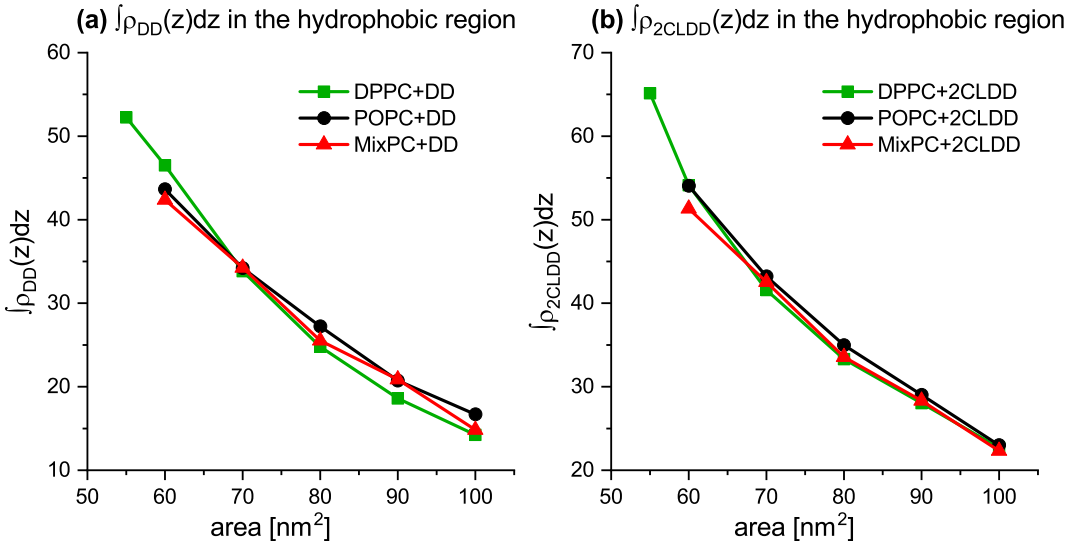

Fig. 3. Integrals of density profiles of DD (a) and 2CLDD (b) molecules in the hydrophobic region (see section 3.2.1 of the main text for details).

outermost H atoms) are equal to *c.a.* 0.5 × 0.9 nm. On the other hand, at the areas 100–80 nm^2, average distance between C22 and C29 atoms in POPC equals to *c.a.* 0.75 nm and that between C210 and C218 atoms equals to *c.a.* 0.85 nm. So DD molecules are small enough to fill the empty spaces created by the kinks in *sn*-2 chains of POPC, especially when they are oriented perpendicularly to monolayer normal. They usually locate under the kink and are roofed over by *sn*-2 chains. Snapshots showing examples of such structures for POPC + DD and MixPC + DD monolayers are presented in Fig. 4a–d. This behavior changes in highly compressed states, in which DD molecules reside deeper in DPPC + DD monolayer than in POPC + DD or MixPC + DD monolayers. This is because in POPC + DD or MixPC + DD systems surface pressure is much higher than in DPPC + DD system, because the latter forms LC phase at low surface areas.

Although in two-component DPPC + DD and POPC + DD systems the effect described above may seem rather small, it has some important consequences for the three component MixPC + DD monolayer. Namely, DD molecules preferentially locate in vicinity of POPC rather than DPPC. In order to confirm this observation we have calculated the average number of carbon atoms belonging to either DPPC or POPC lipid chains in the first coordination shell of DD molecules. The results are presented in Fig. 5a. It can be seen that at all surface areas there are more carbon atoms from POPC chains around DD molecules than from DPPC chains.

Due to their small size, DD molecules maintain high mobility in the monolayers, even in the most compressed states. Average distances travelled by dioxin molecules during the last 70 ns of simulations were similar in all three systems, and varied between 6.8 nm at 100 nm^2 and 2.8 at 60 nm^2. Analysis of diffusion coefficients was however difficult, because MSD functions often deviated significantly from linear dependence on time. The reason for that may be connected with formation of small clusters of DD molecules and, in the case of MixPC system, with preference of DD molecules for POPC chains.

To examine what is the influence of DD molecules on the properties of hydrophobic parts of the monolayers order parameters (S_{mol}) can be analyzed. S_{mol} parameters are related to deuterium order parameters, as explained in equations (3) and (4) in Materials and Methods Section. They attain values close to zero for disordered lipid chains, with large number of gauche defects. Maximum values of 1.0 are achieved for all-trans conformations, with lipid chains directed parallel to monolayer normal. In order to differentiate between the condensing and locally ordering effects mentioned in the previous section, lipids in each monolayer were divided in two groups: those close and far from DD molecules. Lipids with any atoms within 0.5 nm distance from dioxin molecules were included in the first group. The remaining lipids were assigned to the second group. S_{mol} parameters were calculated in each group individually. Results obtained for *sn*-2 chains in DPPC + DD, POPC + DD and MixPC + DD monolayers are presented in panels (a)–(d) of Fig. 6. Some complementary information concerning lipid ordering can also be obtained from distributions of tilt angles between lipid chains and monolayer normal or distances between the first (C22) and last (C216 or C218) carbon atoms in the chains. Results of such calculations are shown in Fig. S5 and S6 and Table S2 of Supplementary Materials.

Fig. 6 shows that in LE phase lipid ordering due to compression is reflected in gradual increase of S_{mol} values. In the case of DPPC monolayer order parameters drop when LC phase is formed (at 60 and 55 nm^2). This behavior is connected with uniform tilt of the chains, *i.e.* lipid chains are in all-trans conformations but due to

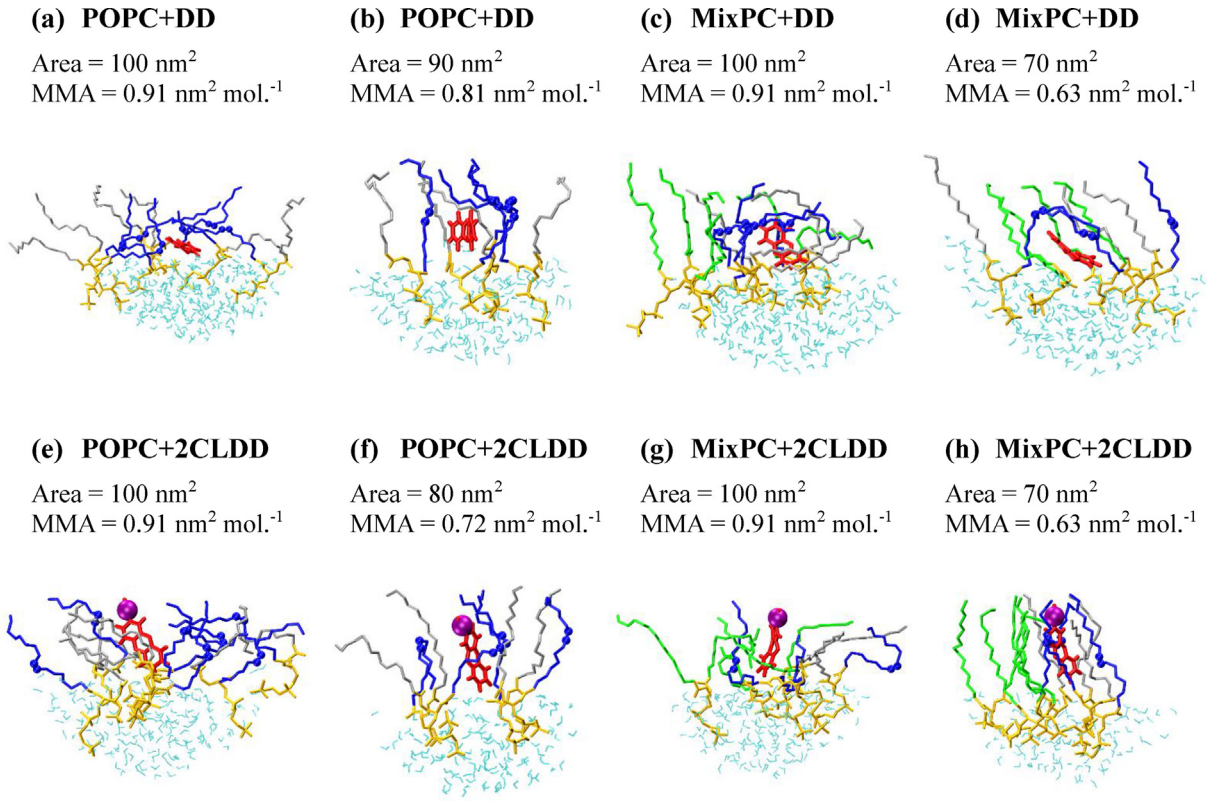

Fig. 4. Snapshots from the recorded trajectories illustrating the way in which lipid chains arrange around DD (panels a–d) and 2CLDD (panels e–h) molecules. Color code: DPPC lipid chains (*sn*-1 and *sn*-2, only C atoms) – green, *sn*-1 chains of POPC (only C atoms) – grey, *sn*-2 chains of POPC (only C atoms) – blue, C9 and C10 atoms (double bond) in *sn*-2 chains of POPC are highlighted with blue balls, headgroup atoms – yellow, DD and 2CLDD – red, Cl atoms in 2CLDD – purple balls, water – cyan.

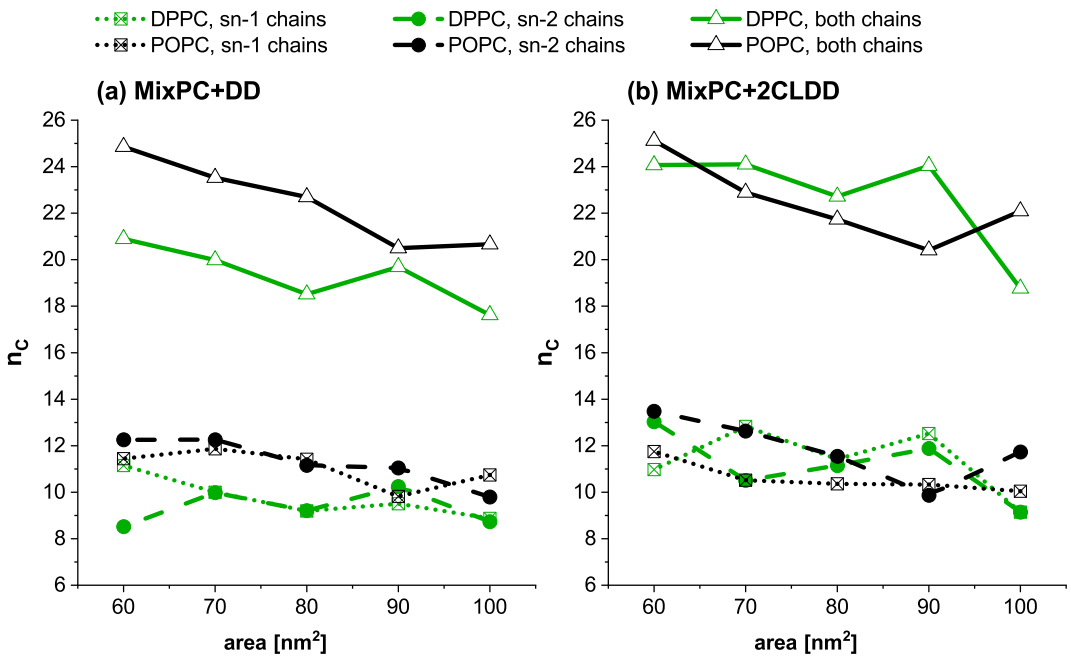

Fig. 5. Average number of carbon atoms from lipid chains in the first coordination shell of dioxin molecules in MixPC + DD (a) and MixPC+2CLDD (b) monolayers as a function of surface area.

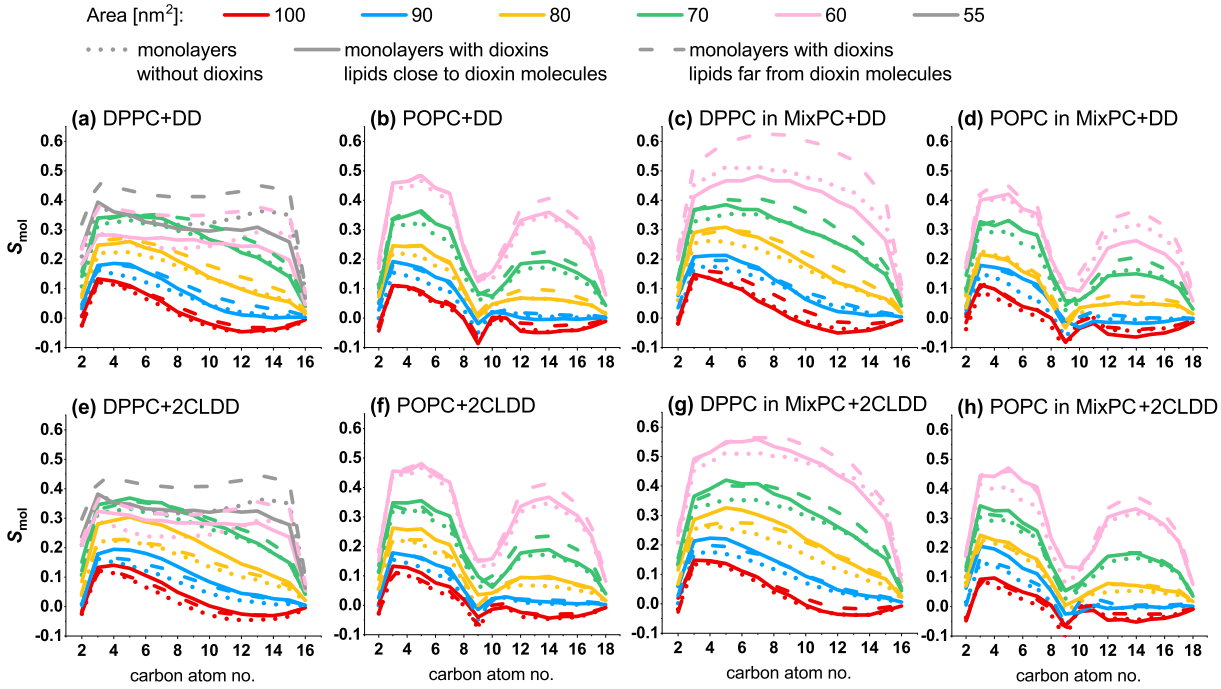

Fig. 6. Order parameters for *sn*-2 lipid chains in pure (dotted lines) and dioxin containing systems at various surface areas. Top row (panels a–d) – results for monolayers with DD molecules, bottom row (panels e–h) – results for monolayers with 2CLDD molecules. In systems with dioxins, S_{mol} values were calculated separately for lipids close to (solid lines) and far from (dashed lines) dioxin molecules.

their tilt with respect to monolayer normal S_{mol} parameters do not reach the value of 1.0 (see tilt angle and chain length distributions in Fig. S5 and S6). In the presence of DD molecules further lipid ordering is observed. It is reflected in: increase of order parameters, shift of tilt angle distributions to smaller angles and increase of chain lengths. In all three systems examined here ordering influence is larger for lipids far from DD molecules. This indicates that the source of ordering is condensation, connected with reduction of surface area available to the lipids. This effect is most pronounced for DPPC lipid chains in MixPC + DD system. This observation can be understood in terms of nonidealities in lipid mixing present in MixPC systems and the preference of DD molecules for POPC chains. As a result of this preference surface area of POPC-rich regions increases, which causes additional compression of DPPC-rich

regions in the monolayer.

In the case of lipids close to DD molecules order parameters increase for the carbon atoms from the first half of the chain, *i.e.* in the region where DD molecules are located, and drop in the second half, because these parts of the chains bend in order to cover dioxin molecules. As expected, this behavior is most pronounced for POPC chains in POPC + DD and MixPC + DD systems. The largest influence of DD presence can be observed in DPPC + DD system at the highest compression (60 and 55 nm^2). Presence of dioxin molecules perturbs ordering of neighboring lipid chains and uniform tilt of the remaining chains is blocked. It can be clearly seen in the distribution of tilt angles for lipids far from DD molecules (Fig. S5), which is shifted towards smaller values with respect to pure DPPC monolayer. This change of tilt angle is responsible for the observed increase of S_{mol} parameters in this group. For lipids close to DD molecules order parameters decrease, distribution of tilt angles is broadened, and the distribution of chain lengths is also wider and significantly shifted towards shorter distances with respect to lipids far from the dioxin (see Fig. S6). This indicates that DD molecules have a strong disordering influence on neighboring lipid chains.

In order to examine the influence of DD on lateral lipid arrangement two dimensional radial pair distribution functions between lipid chains were calculated for all three lipidic compositions. Except for the smallest surface areas we did not observed any significant changes in $g(r)$ plots upon dioxin addition. In $g(r)$ function between DPPC chains in MixPC + DD system at 60 nm^2 the height of the first maximum was elevated with respect to MixPC monolayer and the distance between consecutive maxima was shortened (Fig. S7). $g(r)$ functions between POPC chains or DPPC and POPC chains did not follow this trend. Such behavior can be ascribed to either condensing influence of DD molecules or promotion of lipid de-mixing and formation of DPPC aggregates. Since similar effect was not observed at other surface areas we conclude that the first explanation is more probable in this case. DD molecules also did not affect lateral diffusion coefficients of the lipids to a large extent. No unambiguous trends could be elucidated from changes of D values upon dioxin addition (Fig. S8). Changes in average distance travelled by lipid molecules and position autocorrelation functions for lipids also were within the range of calculation errors. It can be concluded that, even at the relatively large concentration examined in this study, DD molecules are too small to affect lateral lipid motions to a considerable extent.

To probe the influence of DD molecules on the headgroup region of the monolayers, we have calculated distributions of tilt angles between the headgroups and monolayer normal, average number of water molecules in the first hydration shell of various headgroups components, thicknesses of headgroups and the interfacial region, and integrals of radial pair distribution functions between N and P atoms. Selected results of these calculations are presented in Fig. S9-S11 of Supplementary Materials. No significant changes in the above mentioned properties were observed upon addition of dioxin molecules to the monolayers.

3.2.2. Monolayers with 2CLDD molecules

Selected snapshots from simulation of monolayers with 2CLDD molecules are gathered in Fig. S12 of Supplementary Materials. From plots of distributions of tilt angles between long molecular axis of 2CLDD and monolayer normal (Fig. 2d–f) it can readily be seen that, in contrast to DD, 2CLDD molecules adopt vertical orientation, with Cl atoms directed towards air, already at the largest surface areas. The distributions exhibit distinct maxima in the range of small values at all surface areas. For all three lipidic compositions the positions of these maxima move from 52 to 57° at 100 nm^2 to 27–30° at 70 nm^2. In POPC + DD and MixPC + DD systems at 60 nm^2 maxima of tilt angle distributions are located at 20°. In the most compressed states of DPPC+2CLDD system (60 and 55 nm^2) maxima move to larger angles (39–40°) because, similarly to DD, 2CLDD molecules tilt together with surrounding lipid chains (maxima of tilt angle distributions for lipid chains in this system appear at c. a. 35°, see Fig. S14). Density profiles along monolayer normal for selected monolayer components at 100 and 60 nm^2 are presented in Fig. S13. They also demonstrate that, although the density of 2CLDD O atoms overlaps with that of lipid carbonyl groups, Cl atoms reside in the hydrophobic part of the monolayers at all surface areas. Similarly to DD, 2CLDD molecules form linear structures in DPPC+2CLDD monolayer in LC phase.

Vertical orientation of 2CLDD molecules is responsible for different behavior of this dioxin in the monolayers and its' influence on the lipids, especially at large surface areas (100-80 nm^2). First of all, 2CLDD molecules in this orientation no longer fit under the kink in *sn*-2 chains of POPC. Their average height, measured as the distance between C10 atom and the lone pair located on the chlorine atom equals to *c.a.* 1.0 nm. It is therefore larger than the length of the two parts of *sn*-2 chains. For this reason POPC chains do not roof over 2CLDD molecules. Instead, at large surface areas, dioxin Cl atoms are exposed directly to vacuum. Examples of such structures for POPC+2CLDD and MixPC+2CLDD are presented in Fig. 4e–h. As a result, the preference of 2CLDD molecules for POPC chains is much less pronounced than in the case of DD. Integrals of density profiles of 2CLDD in the hydrophobic region (Fig. 3b) show that 2CLDD molecules embed to a similar extent in all three monolayers. For the same reason in MixPC+2CLDD system preference of 2CLDD for POPC chains was not observed. As can be seen from Fig. 5b, carbon atoms from DPPC chains outnumber those from POPC chains in the first coordination shell of 2CLDD at 90, 80, and 70 nm^2.

Another consequence of vertical orientation of 2CLDD molecules is their lower mobility with respect to DD. In all three monolayers average distance travelled by 2CLDD molecules during 70 ns period of simulation varies from 6.2 nm at 100 nm^2 to 2.8 nm at 70 nm^2. At 60 nm^2 differences between monolayers emerge. In POPC+2CLDD and MixPC+2CLDD systems, which are in LE phase, average distance travelled by 2CLDD is reduced to *c.a.* 2.0 nm^2. In DPPC+2CLDD system, which is in LC phase, average distance reduces to 1.3 nm at 60 nm^2 and 1.0 at 55 nm^2. Therefore, behavior of 2CLDD molecules follows behavior of lipids to a greater extent than DD molecules.

Similarly to DD containing systems, the influence of 2CLDD on phase behavior of lipid chains can be analyzed via inspection of order parameters and tilt angle or chain length distributions calculated separately for lipids close and far from 2CLDD molecules. S_{mol} parameters calculated for *sn*-2 lipid chains are gathered in panels (e)–(h) of Fig. 6. Distributions of tilt angles between the chains and monolayer normal, as well as distributions of distances between C22 and C216/C218 atoms are presented in Fig. S14 and S15 of Supplementary Materials, respectively. Changes in tilt angle distributions are also summarized in Table S2. It can be seen that at low compression (100-80 nm^2) S_{mol} values for lipids close to dioxin molecules are elevated with respect to lipids far from 2CLDD or pure monolayers. Distributions of tilt angles between lipid chains and monolayer normal also shift to smaller angles for lipids close to 2CLDD than for lipids far from dioxin molecules. Such behavior indicates that, in addition to condensing effect observed previously for DD molecules, 2CLDD has a locally ordering influence on neighboring lipid chains. We did not identify any specific interactions between dioxin molecules and alkyl chains, which could be responsible for the observed increase of lipid ordering. Analysis of the magnitude of nonbonding contributions to the interaction energy between dioxins and lipids reveals that changing H2 hydrogen atom to chlorine lowers van der Waals interaction energy between dioxin and lipids by 20–30 kcal mol^{-1} in each monolayer.

The change in Coulomb energy is smaller and ranges between −4.2 and 1.0 kcal mol^{-1}, depending on surface area. Therefore, the ordering influence of 2CLDD can be ascribed to non-specific van der Waals interactions between chlorine atoms and alkyl chains, and asymmetric structure of 2CLDD which results in its vertical orientation, with small surface area and Cl atoms embedded in the hydrophobic part of the monolayers. Such orientation of dioxin molecules leads to untangling of lipid chains, and in consequence to increased ordering of the monolayer. When the monolayers are compressed, differences between 2CLDD and DD containing systems decrease. From 80 nm^2 the values of S_{mol} parameters follow the same trends as in the monolayers with DD molecules. This indicates that, condensing effect connected with reduction of surface are available to the lipids begins to dominate. Behavior of the most compressed states of DPPC+2CLDD system, is also similar to DPPC + DD monolayer. Namely, uniform tilt of lipid chains is blocked, which leads to increased values of order parameters.

Similarly to the DD containing systems, we did not observe any pronounced effect of 2CLDD presence on lateral lipid arrangement, lateral diffusion coefficients of lipids, or the headgroup region. Plots of two-dimensional radial pair distribution functions between lipid chains (Fig. S7) and lateral lipid diffusion coefficients (Fig. S8) overlapped to within the calculation error with those of monolayers without dioxins. Also, as shown in Fig. S9-S11 of Supplementary Materials, the distributions of tilt angles between the headgroups and monolayer normal, average number of water molecules in the first hydration shell of N, P, and carbonyl O atoms, and integrals of radial pair distribution functions between N and P atoms are almost identical to those observed in monolayers without dioxins or with DD molecules.

3.3. PM-IRRAS measurements

PM-IRRAS spectra recorded for pure MixPC and MixPC + DD systems at $\Pi = 30$ mN m^{-1} are presented in Fig. 7. Results obtained in these experiments are in agreement with observations derived from MD simulations. In the region 2800-3000 cm^{-1}, corresponding to stretching vibrations of aliphatic C—H bonds, two characteristic peaks can be observed (Fig. 7, left panel). Namely, symmetric methylene stretching vibration, $\nu_s(CH_2)$, at *c.a.* 2860-2870 cm^{-1}, and antisymmetric methylene stretching vibration, $\nu_a(CH_2)$, at *c.a.* 2920 cm^{-1}. It can be seen that in MixPC + DD and MixPC+2CLDD systems positions of both $\nu_s(CH_2)$ and $\nu_a(CH_2)$ peaks are shifted towards smaller wavenumbers. Such behavior is characteristic for increased chain ordering. On the other hand, behavior of polar lipid headgroups can be probed by examining spectra in the region 1650-1800 cm^{-1}, where the peak from stretching vibration of lipid carbonyl groups, ν(C═O), appears. The position of this peak reflects the degree of headgroups hydration, in particular H-bonding. As can be seen, no pronounced effect is observed upon DD or 2CLDD addition to the monolayer (Fig. 7, right panel). The above results confirm that DD and 2CLDD molecules influence mostly the hydrophobic part of the monolayer, inducing additional lipid ordering.

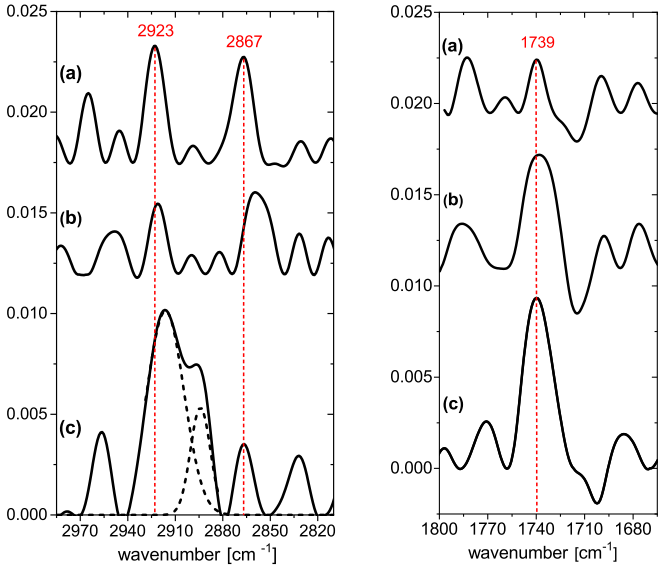

Fig. 7. PM-IRRAS spectra recorded at 30 mN m^{-1} and characteristic vibrational wavenumbers for MixPC (a), MixPC + DD (b), and MixPC+2CLDD (c) systems.

4. Conclusions

In the present study interactions between a lung surfactant model and two dibenzo-*p*-dioxins, namely dibenzo-*p*-dioxin and 2-chlorodibenzo-*p*-dioxin, were examined. Both DD and 2CLDD molecules are relatively small and highly hydrophobic. This study demonstrates that in Langmuir monolayer at high surface pressures both of them attain vertical orientations which correspond to small surface area. For these reasons both DD and 2CLDD accumulate in the monolayer and are hard to remove, even at very large surface pressures. In this aspect their behavior differs from that observed in our previous study for another air pollutant – benzo[a]pyrene (BaP) (Stachowicz-Kusnierz et al., 2017). BaP molecules are larger than dibenzodioxins and in our simulations we observed that they were expelled from DPPC, POPC, and MixPC monolayers at high surface pressures. They were therefore able to cross LS barrier and enter the organism in an uncontrolled manner. This is not the case for DD or 2CLDD molecules. Even though the concentration of 10 mol% considered here is relatively high, all dioxin molecules remained in the monolayers. LS may therefore be recognized as a good barrier for uncontrolled uptake of airborne dioxin molecules into the body.

Behavior of dioxin molecules and their influence on the lipids differ in LE and LC phases. In LE phase they are also different for DD and 2CLDD molecules. At larger MMA, DD and 2CLDD molecules exhibit a common condensing effect on all three monolayers. Its' source is connected with reduction of the surface area available to the lipids, resulting in additional compression of the lipids far from dioxin molecules. In the case of 2CLDD, additional locally ordering influence of dioxin molecules was observed at large MMAs. It resulted from non-specific van der Waals interaction between the chlorine atom and alkyl lipid chains. The increase of interaction energy between dioxin molecules and lipids, when a hydrogen atoms is replaced by chlorine, is in line with the known increase of lipophilicity upon introduction of chlorine atoms to various biologically active molecules, be they drugs (Gerebtzoff et al., 2004) or organic pollutants (El-Shahawi et al., 2010). Due to favorable van der Waals interactions between Cl atom and lipid chains and asymmetric structure 2CLDD attain vertical orientations in the monolayer already at low compression. This in turn leads to untangling of lipid chains and increases ordering of the monolayer. On the other hand, DD molecules at low compression orient flatwise on the border between hydrophilic and hydrophobic parts of the monolayers. Such orientation is favored entropically because it preserves high entropy of tangles lipid chains. As a result DD molecules occupy large surface area in the monolayer. In consequence they display preference towards unsaturated lipid chains of POPC – their small size enables them to locate in void spaces created in the hydrophobic part of the monolayer by kinks in unsaturated chains.

In LC phase formed by DPPC monolayer at low surface areas the

influence of both dioxins on the lipids is similar – they strongly perturb ordering of neighboring lipid chains. Their presence also blocks alignment and uniform tilt of the remaining chains. However, in the case of DD it can be expected that this effect will not have significant biological consequences for functioning of LS, since DD molecules preferentially locate in vicinity of POPC, *i.e.* in LE phase. As a final conclusion, it can be stated that adsorption of dibenzodioxins examined here is a good example of how well LS manages with small, hydrophobic impurities adsorbed from air. The role of POPC seems especially important for this purpose. By accommodating pollutant molecules in void spaces in the hydrophobic part of the monolayer POPC precludes them from perturbing formation of LC phase which is crucial for achievement of near-zero surface tension. Also, while cycling between the surface and surface associate reservoirs, material from LE phase is subject to surfactant repair processes, such as detachment from the surface and clearance, *e.g.* by macrophages (Wright, 1990; Agassandian and Mallampalli, 2013; Olmeda et al., 2017). In this manner dibenzodioxins could be intercepted by the immune system of the organism.

Conflict of interest

There is no conflict of interest to declare.

Acknowledgements

This work was supported by the Polish National Science Centre, Project No. UMO-2014/13/B/ST4/04995. Calculations were performed at Faculty of Chemistry of Jagiellonian University on a computer cluster purchased with the financial support from the European Regional Development Fund in the framework of the Polish Innovation Economy Operational Program (Contract No. OIG.02.01.00-12-023/08) and on PL-Grid infrastructure at ACK CYFRONET with the support of the "HPC Infrastructure for Grand Challenges of Science and Engineering" project.

Appendix A. Supplementary data

Supplementary data related to this article can be found at https://doi.org/10.1016/j.chemosphere.2019.124850.

References

Abraham, M.J., Murtola, T., Schulz, R., Páll, S., Smith, J.C., Hess, B., Lindahl, E., 2015. GROMACS: high performance molecular simulations through multi-level parallelism from laptops to supercomputers. SoftwareX 1–2, 19–25.
Agassandian, M., Mallampalli, R.K., 2013. Surfactant phospholipid metabolism. Biochim. Biophys. Acta 1831, 612–625.
Baoukina, S., Monticelli, L., Marrink, S.J., Tieleman, D.P., 2007. Pressure-area isotherm of a lipid monolayer from molecular dynamics simulations. Langmuir 23, 12617–12623.
Baoukina, S., Mendez-Villuendas, E., Tieleman, D.P., 2012. Molecular view of phase coexistence in lipid monolayers. J. Am. Chem. Soc. 134, 17543–17553.
Ceccarelli, M., Germani, R., Massari, S., Petit, C., Nurisso, A., Wolfender, J.L., Goracci, L., 2015. Phospholipidosis effect of drugs by adsorption into lipid monolayers. Colloids Surfaces B Biointerfaces 136, 175–184.
Comission, E., 2001. Community strategy for dioxins, furans and polychlorinated biphenyls. Off. J. Eur. Communities 332, 2–18.
Czapla, K., Korchowiec, B., Orlof, M., Magnieto, J.R., Rogalska, E., 2011. Enzymatic probing of model lipid membranes: phospholipase A2 activity toward monolayers modified by oxicam NSAIDs. J. Phys. Chem. B 115, 9290–9298.
Darden, T., York, D., Pedersen, L., 1993. Particle mesh Ewald: an N·log(N) method for Ewald sums in large systems. J. Chem. Phys. 98, 10089–10092.
Davy, C.W., 2004. Legislation with respect to dioxins in the workplace. Environ. Int. 30, 219–233.
Dopico, M., Gomez, A., 2015. Review of the current state and main sources of dioxins around the world. J. Air Waste Manag. Assoc. 65, 1033–1049.
Duncan, S.L., Larson, R.G., 2008. Comparing experimental and simulated pressure-area isotherms for DPPC. Biophys. J. 94, 2965–2986.
Duncan, S.L., Larson, R.G., 2010. Folding of lipid monolayers containing lung surfactant proteins SP-B_{1-25} and SP-C studied via coarse-grained molecular dynamics simulations. Biochim. Biophys. Acta 1798, 1632–1650.
Eftaiha, A.F., Brunet, S.M., Paige, M.F., 2012. Thermodynamic and structural characterization of a mixed perfluorocarbon-phospholipid ternary monolayer surfactant system. J. Colloid Interface Sci. 368, 356–365.
El-Shahawi, M.S., Hamza, A., Bashammakh, A.S., Al-Saggaf, W.T., 2010. An overview on the accumulation, distribution, transformations, toxicity and analytical methods for the monitoring of persistent organic pollutants. Talanta 80, 1587–1597.
Engelskirchen, S., 2007. The pseudo-binary pulmonary surfactant system. Curr. Opin. Colloid Interface Sci. 12, 68–74.
Feller, S.E., Zhang, Y.H., Pastor, R.W., Brooks, B.R., 1995. Constant-pressure molecular-dynamics simulation - the Langevin piston method. J. Chem. Phys. 103, 4613–4621.
Frisch, M.J., Trucks, G.W., Schlegel, H.B., Scuseria, G.E., Robb, M.A., Cheeseman, J.R., Scalami, G., Barone, V., Menucci, B., Petersson, G.A., Nakatsuji, H., Caricato, M., Li, X., Hratchian, H.P., Izmaylov, A.F., Bloino, J., Zheng, G., Sonnenberg, J.L., Hada, M., Ehara, M., Toyota, K., Fukuda, R., Hasegawa, J., Ishida, M., Nakajima, T., Honda, Y., Kitao, O., Nakai, H., Vreven, T., Montgomery Jr., J.A., Peralta, J.E., Ogliaro, F., Bearpark, M., Heyd, J., Brothers, E., Kudin, K.N., Staroverov, V.N., Kobayashi, R., Normand, J., Raghavachari, K., Rendell, A., Burant, J.C., Iyengar, S.S., Tomasi, J., Cossi, M., Rega, N., Millam, J.M., Klene, M., Knox, J.E., Cross, J.B., Bakken, V., Adamo, C., Jaramillo, J., Gomperts, R., Stratmann, R.E., Yazyev, O., Austrin, A.J., Cammi, R., Pomelli, C., Ochterski, W., Martin, R.L., Morokuma, K., Zakrzewski, V.G., Voth, G.A., Salvador, P., Dannenberg, J.J., Dapprich, S., Daniels, A.D., Farkas, O., Foresman, J.B., Ortiz, J.V., Cioslowski, J., Fox, D.J., 2009. Gaussian 09, Revision A.02. Gaussian Inc., Wallingford CT.
Gerebtzoff, G., Li-Blatter, X., Fischer, H., Frentzel, A., Seelig, A., 2004. Halogenation of drugs enhances membrane binding and permeation. Chembiochem 5, 676–684.
Goerke, J., 1998. Pulmonary surfactant: functions and molecular composition. Biochim. Biophys. Acta 1408, 79–89.
Goerke, J., Gonzalez, J., 1981. Temperature dependence of dipalmitoyl phosphatidylcholine monolayer stability. J. Appl. Physiol. Respir. Environ. Exerc. Physiol. 51, 1108–1114.
Gullett, B.K., Wikstrom, E., 2000. Mono- to tri-chlorinated dibenzodioxin (CDD) and dibenzofuran (CDF) congeners/homologues as indicators of CDD and CDF emissions from municipal waste and waste/coal combustion. Chemosphere 40, 1015–1019.
Han, Y., Liu, W., Hansen, H.C.B., Chen, X., Liao, X., Li, H., Wang, M., Yan, N., 2016. Influence of long-range atmospheric transportation (LRAT) on mono-to octachlorinated PCDD/Fs levels and distributions in soil around Qinghai Lake, China. Chemosphere 156, 143–149.
Hess, B., Bekker, H., Berendsen, H.J.C., Fraaije, J.G.E.M., 1997. LINCS: a linear constraint solver for molecular simulations. J. Comput. Chem. 18, 1463–1472.
Humphrey, W., Dalke, A., Schulten, K., 1996. VMD: visual molecular dynamics. J. Mol. Graph. 14, 33–38.
Huynh, L., Perrot, N., Beswick, V., Rosilio, V., Curmi, P.A., Sanson, A., Jamin, N., 2014. Structural properties of POPC monolayers under lateral compression: computer simulations analysis. Langmuir 30, 564–573.
Izadi, S., Anandakrishnan, R., Onufriev, A.V., 2014. Building water models: a different approach. J. Phys. Chem. Lett. 5, 3863–3871.
Javanainen, M., Lamberg, A., Cwiklik, L., Vattulainen, I., Ollila, O.H.S., 2018. Atomistic model for nearly quantitative simulations of Langmuir monolayers. Langmuir 34, 2565–2572.
Jorgensen, W.L., Chandrasekhar, J., Madura, J.D., Impey, R.W., Klein, M.L., 1983. Comparison of simple potential functions for simulating liquid water. J. Chem. Phys. 79, 926–935.
Keating, E., Zuo, Y.Y., Tadayyon, S.M., Petersen, N.O., Possmayer, F., Veldhuizen, R.A., 2012. A modified squeeze-out mechanism for generating high surface pressures with pulmonary surfactant. Biochim. Biophys. Acta 1818, 1225–1234.
Klauda, J.B., Venable, R.M., Freites, J.A., O'Connor, J.W., Tobias, D.J., Mondragon-Ramirez, C., Vorobyov, I., MacKerell Jr., A.D., Pastor, R.W., 2010. Update of the CHARMM all-atom additive force field for lipids: validation on six lipid types. J. Phys. Chem. B 114, 7830–7843.
Knecht, V., Muller, M., Bonn, M., Marrink, S.J., Mark, A.E., 2005. Simulation studies of pore and domain formation in a phospholipid monolayer. J. Chem. Phys. 122, 024704.
Korchowiec, B., Corvis, Y., Viitala, T., Feidt, C., Guiavarch, Y., Corbier, C., Rogalska, E., 2008. Interfacial approach to polyaromatic hydrocarbon toxicity: phosphoglyceride and cholesterol monolayer response to phenantrene, anthracene, pyrene, chrysene, and benzo[a]pyrene. J. Phys. Chem. B 112, 13518–13531.
Korchowiec, B., Korchowiec, J., Hato, M., Rogalska, E., 2011. Glycolipid-cholesterol monolayers: towards a better understanding of the interaction between the membrane components. Biochim. Biophys. Acta 1808, 2466–2476.
Korchowiec, B., Gorczyca, M., Korchowiec, J., Rubio-Magnieto, J., Lotfallah, A.H., Luis, S.V., Rogalska, E., 2016a. Structure - membrane activity relationship in a family of peptide-based gemini amphiphiles: an insight from experimental and theoretical model systems. Colloids Surfaces B Biointerfaces 146, 54–62.
Korchowiec, B., Gorczyca, M., Rogalska, E., Regnouf-de-Vains, J.B., Mourer, M., Korchowiec, J., 2016b. The selective interactions of cationic tetra-p-guanidinoethylcalix[4]arene with lipid membranes: theoretical and experimental model studies. Soft Matter 12, 181–190.
Kulkarni, P.S., Crespo, J.G., Afonso, C.A., 2008. Dioxins sources and current remediation technologies-a review. Environ. Int. 34, 139–153.

Lai, C.C., Yang, S.H., Finlayson-Pitts, B.J., 1994. Interactions of monolayers of unsaturated phosphocholines with ozone at the air-water interface. Langmuir 10, 4637–4644.
Lee, Y.L., Lin, J.Y., Chang, C.H., 2006. Thermodynamic characteristics and Langmuir-Blodgett deposition behavior of mixed DPPA/DPPC monolayers at air/liquid interfaces. J. Colloid Interface Sci. 296, 647–654.
Liu, W., Tian, Z., Li, H., Xie, H., Xiao, K., Li, C., Tang, C., Zheng, M., 2013. Mono- to octachlorinated PCDD/Fs in stack gas from typical waste incinerators and their implications on emission. Environ. Sci. Technol. 47, 9774–9780.
Mayne, C.G., Saam, J., Schulten, K., Tajkhorshid, E., Gumbart, J.C., 2013. Rapid parameterization of small molecules using the Force Field Toolkit. J. Comput. Chem. 34, 2757–2770.
Munden, J., Swarbrick, J., 1973. Effect of spreading solvent on monolayer characteristics of dipalmitoyl lecithin. J. Colloid Interface Sci. 42, 657–659.
Nisoh, N., Karttunen, M., Monticelli, L., Wong-ekkabut, J., 2015. Lipid monolayer disruption caused by aggregated carbon nanoparticles. RSC Adv. 5, 11676–11685.
Olmeda, B., Martinez-Calle, M., Perez-Gil, J., 2017. Pulmonary surfactant metabolism in the alveolar airspace: biogenesis, extracellular conversions, recycling. Ann. Anat. 209, 78–92.
Olzynska, A., Zubek, M., Roeselova, M., Korchowiec, J., Cwiklik, L., 2016. Mixed DPPC/POPC monolayers: all-atom molecular dynamics simulations and Langmuir monolayer experiments. Biochim. Biophys. Acta 1858, 3120–3130.
Orgeig, S., Hiemstra, P.S., Veldhuizen, E.J., Casals, C., Clark, H.W., Haczku, A., Knudsen, L., Possmayer, F., 2010. Recent advances in alveolar biology: evolution and function of alveolar proteins. Respir. Physiol. Neurobiol. 173 (Suppl. l), S43–S54.
Perez-Gil, J., 2008. Structure of pulmonary surfactant membranes and films: the role of proteins and lipid-protein interactions. Biochim. Biophys. Acta 1778, 1676–1695.
Phillips, J.C., Braun, R., Wang, W., Gumbart, J., Tajkhorshid, E., Villa, E., Chipot, C., Skeel, R.D., Kale, L., Schulten, K., 2005. Scalable molecular dynamics with NAMD. J. Comput. Chem. 26, 1781–1802.
Piknova, B., Schief, W.R., Vogel, V., Discher, B.M., Hall, S.B., 2001. Discrepancy between phase behavior of lung surfactant phospholipids and the classical model of surfactant function. Biophys. J. 81, 2172–2180.
Prenner, E., Honsek, G., Honig, D., Mobius, D., Lohner, K., 2007. Imaging of the domain organization in sphingomyelin and phosphatidylcholine monolayers. Chem. Phys. Lipids 145, 106–118.
Roke, S., Schins, J., Muller, M., Bonn, M., 2003. Vibrational spectroscopic investigation of the phase diagram of a biomimetic lipid monolayer. Phys. Rev. Lett. 90, 128101.
Schürch, S., 1982. Surface tension at low lung volumes: dependence on time and alveolar size. Respir. Physiol. 48, 339–355.
Schurch, S., Goerke, J., Clements, J.A., 1976. Direct determination of surface tension in the lung. Proc. Natl. Acad. Sci. U. S. A. 73, 4698–4702.
Serrano, A.G., Perez-Gil, J., 2006. Protein-lipid interactions and surface activity in the pulmonary surfactant system. Chem. Phys. Lipids 141, 105–118.
Shen, Y., Tang, Y., Xie, A., Zhu, J., Li, S., Zhang, Y., 2006. Studies on behaviors of dipalmitoylposphatidylcholine and bilirubin in mixed monolayer at the air/water interface. Appl. Surf. Sci. 252, 5861–5867.
Soteras Gutierrez, I., Lin, F.Y., Vanommeslaeghe, K., Lemkul, J.A., Armacost, K.A., Brooks 3rd, C.L., MacKerell Jr., A.D., 2016. Parametrization of halogen bonds in the CHARMM general force field: improved treatment of ligand-protein interactions. Bioorg. Med. Chem. 24, 4812–4825.
Stachowicz-Kusnierz, A., Trojan, S., Cwiklik, L., Korchowiec, B., Korchowiec, J., 2017. Modeling lung surfactant interactions with benzo[a]pyrene. Chem. Eur J. 23, 5307–5316.
Tavakoly Sany, S.B., Hashim, R., Salleh, A., Rezayi, M., Karlen, D.J., Razavizadeh, B.B., Abouzari-Lotf, E., 2015. Dioxin risk assessment: mechanisms of action and possible toxicity in human health. Environ. Sci. Pollut. Res. 22, 19434–19450.
Van den Berg, M., Birnbaum, L.S., Denison, M., De Vito, M., Farland, W., Feeley, M., Fiedler, H., Hakansson, H., Hanberg, A., Haws, L., Rose, M., Safe, S., Schrenk, D., Tohyama, C., Tritscher, A., Tuomisto, J., Tysklind, M., Walker, N., Peterson, R.E., 2006. The 2005 World Health Organization re-evaluation of human and mammalian toxic equivalency factors for dioxins and dioxin-like compounds. Toxicol. Sci. 93, 223–241.
Vanommeslaeghe, K., Hatcher, E., Acharya, C., Kundu, S., Zhong, S., Shim, J., Darian, E., Guvench, O., Lopes, P., Vorobyov, I., Mackerell Jr., A.D., 2010. CHARMM general force field: a force field for drug-like molecules compatible with the CHARMM all-atom additive biological force fields. J. Comput. Chem. 31, 671–690.
Vargaftik, N.B., Volkov, B.N., Voljak, L.D., 1983. International tables of the surface tension of water. J. Phys. Chem. Ref. Data 12, 817–820.
Vega, C., de Miguel, E., 2007. Surface tension of the most popular models of water by using the test-area simulation method. J. Chem. Phys. 126, 154707.
Veldhuizen, R., Nag, K., Orgeig, S., Possmayer, F., 1998. The role of lipids in pulmonary surfactant. Biochim. Biophys. Acta 1408, 90–108.
White, S.S., Birnbaum, L.S., 2009. An overview of the effects of dioxins and dioxin-like compounds on vertebrates, as documented in human and ecological epidemiology. J. Environ. Sci. Health C Environ. Carcinog. Ecotoxicol. Rev. 27, 197–211.
World Health Organization, 1997. IARC monographs on the evaluation of carcinogenic risk to humans. IARC Monographs 69, 343.
Wright, J.R., 1990. Clearance and recycling of pulmonary surfactant. Am. J. Physiol. Lung Cell Mol. Physiol. 259, L1–L12.
Wüstneck, N., Wüstneck, R., Fainerman, V.B., Pison, U., Miller, R., 2000. Investigation of over-compressed spread L-dipalmitoyl phosphatidylcholine films and the influence of solvent vapour in the gas phase on Π/A isotherms measured by using the captive bubble technique. Colloid. Surf. Physicochem. Eng. Asp. 164, 267–278.
Zakharov, V.V., Brodskaya, E.N., Laaksonen, A., 1998. Surface properties of water clusters: a molecular dynamics study. Mol. Phys. 95, 203–209.
Zhang, H., Wang, Y.E., Fan, Q., Zuo, Y.Y., 2011. On the low surface tension of lung surfactant. Langmuir 27, 8351–8358.
Zhang, X., Zheng, M., Liu, G., Zhu, Q., Dong, S., Zhang, H., Wang, X., Xiao, K., Gao, L., Liu, W., 2016. A comparison of the levels and particle size distribution of lower chlorinated dioxin/furans (mono- to tri-chlorinated homologues) with those of tetra- to octa-chlorinated homologues in atmospheric samples. Chemosphere 151, 55–58.
Zuo, Y.Y., Veldhuizen, R.A., Neumann, A.W., Petersen, N.O., Possmayer, F., 2008. Current perspectives in pulmonary surfactant-inhibition, enhancement and evaluation. Biochim. Biophys. Acta 1778, 1947–1977.